Journal Pre-proof

Visible and UV photocatalysis of aqueous perfluorooctanoic acid by TiO_2 and peroxymonosulfate: Process kinetics and mechanistic insights

Bentuo Xu, Mohammad Boshir Ahmed, John L. Zhou, Ali Altaee

PII: S0045-6535(19)32606-2

DOI: https://doi.org/10.1016/j.chemosphere.2019.125366

Reference: CHEM 125366

To appear in: *ECSN*

Received Date: 5 August 2019

Revised Date: 4 November 2019

Accepted Date: 12 November 2019

Please cite this article as: Xu, B., Ahmed, M.B., Zhou, J.L., Altaee, A., Visible and UV photocatalysis of aqueous perfluorooctanoic acid by TiO_2 and peroxymonosulfate: Process kinetics and mechanistic insights, *Chemosphere* (2019), doi: https://doi.org/10.1016/j.chemosphere.2019.125366.

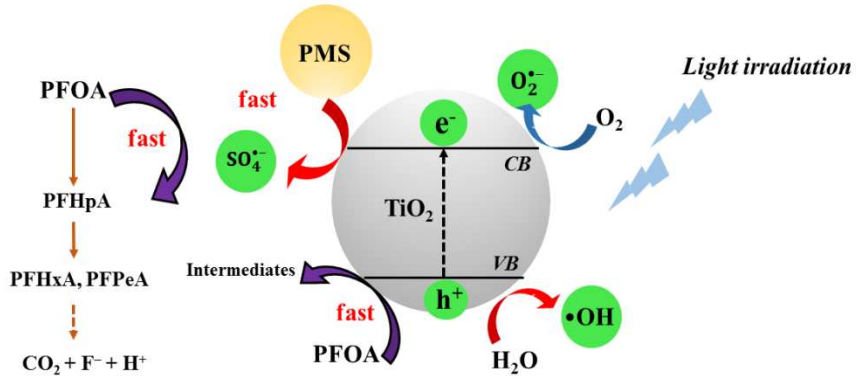

Visible and UV photocatalysis of aqueous perfluorooctanoic acid by TiO_2 and peroxymonosulfate: process kinetics and mechanistic insights

Bentuo Xu[a,b], Mohammad Boshir Ahmed[a], John L. Zhou[a*], Ali Altaee[a]

[a] Centre for Green Technology, School of Civil and Environmental Engineering, University of Technology Sydney, 15 Broadway, NSW 2007, Australia

[b] School of Life and Environmental Science, Wenzhou University, Wenzhou 325035, China

Corresponding author:

Prof John L. Zhou

Centre for Green Technology

School of Civil and Environmental Engineering

University of Technology Sydney

15 Broadway, NSW 2007

Australia

Email: junliang.zhou@uts.edu.au

Abstract

The global occurrence and adverse environmental impacts of perfluorooctanoic acid (PFOA) have attracted wide attention. This study focused on the PFOA photodegradation by using photocatalyst TiO_2 with peroxymonosulfate (PMS) activation. Aqueous PFOA (50 mg L^{-1}) at the pH 3 was treated by TiO2/PMS under 300 W visible light (400-770 nm) or 32 W UV light (254 nm and 185 nm). The addition of PMS induced a significant degradation of PFOA under powerful visible light compared with sole TiO_2. Under visible light, 0.25 g L^{-1} TiO_2 and 0.75 g L^{-1} PMS in the solution with the initial pH 3 provided optimum condition which achieved 100% PFOA removal within 8 h. Under UV light irradiation at 254 nm and 185 nm wavelength, TiO_2/PMS presented excellent performance of almost 100% removal of PFOA within 1.5 h, attributed to the high UV absorbance by the photocatalyst. The intermediates analysis showed that PFOA was degraded from a long carbon chain PFOA to shorter chain intermediates in a stepwise manner. Furthermore, scavenger experiments indicated that $SO_4^{\bullet-}$ radicals from PMS and photogenerated holes from TiO_2 played an essential role in degrading PFOA. The presence of organic compounds in real wastewater reduced the degradation efficacy of PFOA by 18-35% in visible/TiO_2/PMS system. In general, TiO_2/PMS could be an ideal and effective photocatalysis system for the degradation of PFOA from wastewater using either visible or UV light source.

Keywords: Perfluorooctanoic acid; Peroxymonosulfate; Photocatalysis; Sulfate radicals; Visible light

1. Introduction

Perfluoroalkyl substances (PFAS) have been extensively used in industry and consumer products since the 1950s (Janousek et al., 2019). Consequently, some PFAS, in particular perfluorooctanoic acid (PFOA), are widely detected in the aquatic environment to reach μg L^{-1} and even up to mg L^{-1} concentrations. For instance, Valsecchi et al. (2015) reported that the concentration of PFOA in the surface water of Bormida River, Italy ranged from 0.253 to 6.468 μg L^{-1}, with the mean value of 1.613 μg L^{-1}. In studying PFAS occurrence in surface water within a 10 km radius from a mega-fluorochemical industrial park, Liu et al. (2016) found that PFOA was at a severe contamination level with the concentration ranging from 0.0386 to 1707 μg L^{-1}. These levels constitute human health risks, which may lead to growth and reproduction toxicity, liver injury and even cancer from PFOA exposure (Bassler et al., 2019; Behr et al., 2018; Hurley et al., 2018). In February 2019, the United States Environmental Protection Agency (USEPA) established a multi-media, multi-program, national communication and research plan to address emerging environmental challenge from PFAS (https://www.epa.gov/pfas). Therefore, it is increasingly urgent to develop novel technologies with high efficacy and low cost for PFAS degradation.

Advanced oxidation processes (AOPs) such as ozonation, Fenton, ferrate and photocatalysis are widely used to degrade organic pollutants through free radicals, as reviewed by Sornalingam et al. (2016). AOPs based on hydroxyl radicals are effective for treating endocrine disrupting chemicals such as bisphenol A (Xiao et al., 2017), while sulfate radicals are effective in the degradation of pharmaceuticals in water (Gao et al., 2019). Of different AOPs, heterogeneous photocatalysis has drawn significant scientific attention to be applied for the treatment of organic pollutants including PFAS (Xu et al., 2017; Xu et al., 2018). Of different photocatalysts, titanium dioxide (TiO_2) has proven to be one of the most promising semiconductors for heterogeneous photocatalysis due to its wide band gap (3.14 eV), nontoxicity and long-term photostability (Yoo et al., 2018; Zhang et al., 2019). Hence,

TiO_2 is widely used as co-catalyst synthesized with other materials during the photocatalytic process (Wang and Zhang, 2011). For example, Chen et al. (2012) investigated the accelerated TiO_2 (1000 mg L^{-1}) photodegradation of Acid Oange 7 (AO7) under visible light mediated by 614 mg L^{-1} of peroxymonosulfate (PMS). PMS, derived from the Oxone ($KHSO_5 \cdot 0.5KHSO_4 \cdot 0.5K_2SO_4$), as an environmentally friendly oxidant, could produce sulfate radicals ($SO_4^{\bullet -}$) in the solution and induce a remarkable synergistic effect in the combined TiO_2/PMS system (Feng et al., 2018; Jo et al., 2018). As a consequence, AO7 was fully degraded by TiO_2/PMS within 1.5 h, while only about 60% AO7 was removal by TiO_2 only (Chen et al., 2012). In another study, Khan et al. (2017) found that TiO_2/PMS (230/61 mg L^{-1}) could efficiently degrade lindane by visible light with 100% removal within 4 h. It has some obvious drawbacks such as the recombination of photo-generated charge carriers, which reduces the overall quantum efficiency (Cao et al., 2016; Pan et al., 2013).

For PFAS photodegradation, Park et al. (2018) synthesized graphene oxide/TiO_2 nanotubes array as catalysts irradiated by UV light, which achieved 83% PFOA degradation within 4 h. Wu et al. (2018) used ZnO-reduced graphene oxide combined with persulfate oxidation under UV light irradiation for PFOA degradation, and observed that almost 100% PFOA was removed within 4 h. However, such methods have some potential drawbacks in relation to real world applications. Firstly, these catalysts are commonly synthesized under certain conditions (i.e. high temperature and specific precursors), which unavoidably increase the cost and operation difficulty. Secondly, UV light was often the indispensable light source in the photocatalytic system to active the photocatalytic degradation of pollutants (Hao et al., 2019). At ground level, 44% of the sunlight energy is in the visible range, with only 3% in the ultraviolet range. Thus, it is difficult to utilize UV light from sunlight as photodegradation energy source, and the extra UV energy has to be provided for PFAS degradation, with UV-based treatment technologies.

The aim of this work was to investigate the feasibility of using TiO_2 with PMS for PFOA removal under visible light as a green technology. The objectives were to determine the kinetics and extent of PFOA photodegradation under visible light, the effects of catalyst dosage and initial solution pH on photodegradation, the reaction intermediates of PFOA photodegradation in the visible/TiO_2/PMS system, and the degradation pathway via the scavenger experiments. For comparison, the photodegradation was also conducted under UV light to evaluate the photocatalytic efficacy. In addition, PFOA photodegradation performance by TiO_2/PMS catalyst in real wastewater samples with a highly complex matrix was explored.

2. Materials and methods

2.1. Materials

The chemical structure of common PFAS is shown in **Fig. S1**. PFOA ($C_7F_{15}COOH$, 95%), perfluoroheptanoic acid (PFHpA, $C_6F_{13}COOH$, 99%), perfluorohexanoic acid (PFHxA, $C_5F_{11}COOH$, ≥ 97%), perfluoropentanoic acid (PFPeA, C_4F_9COOH, 97%), perfluorobutanoic acid (PFBA, C_3F_7COOH, 98%), pentafluoropropionic acid (PFPA, C_2F_5COOH, 97%) and trifluoroacetic acid (TFA, CF_3COOH, ≥ 99%) were obtained from Sigma-Aldrich, Australia. Evonik, Germany kindly supplied TiO_2 (P25). Oxone ($2KHSO_5 \cdot KHSO_4 \cdot K_2SO_4$, 97% purity) was purchased from Sigma-Aldrich, Australia. The scavengers of *tert*-butanol (*t*-BuOH), disodium ethylenediaminetetraacetate (EDTA-Na_2) and benzoquinone (BQ) were also bought from Sigma-Aldrich. All chemicals in this study were used as received, and all the solutions were prepared using ultra-pure water obtained from Milli-Q water system.

2.2. Photocatalytic degradation of PFOA

All experiments were conducted in a cylindrical reactor vessel filled with 200 mL of PFOA solution (50 mg L^{-1}) and mixed continuously using magnetic stirring. The concentration of 50 mg L^{-1} was comparatively higher than that in the most contaminated water, which was also used as the initial concentration in the previous literature (Panchangam

et al., 2009). PFOA aqueous solution was prepared by diluting the stock solution in the beaker. The diluting water could be ultra-pure water or wastewater samples (influent and effluent) taken from a municipal sewage treatment plant in Sydney, Australia. The influent went through physical settlement and biodegradation and discharged as effluent. TiO_2 and PMS were added at the concentrations of 0.025-0.30 mg L^{-1} and 0.25-1.0 mg L^{-1}, respectively and stirred for 0.5 h under darkness to achieve adsorption-desorption equilibrium. The effect of solution pH on PFOA photodegradation was assessed by varying solution pH at 3, 5, 7 and 10.

The visible light source was provided by a 300 W Xenon lamp (HSX-F500, NBeT Company, China) positioned 38 cm above the liquid surface inside the reactor as shown in **Fig. S2**. A filter was used to remove wavelengths shorter than 400 nm so the wavelength of the light source was confined to 400–770 nm. The electric current was 20 A and light intensity in the centre of the reactive solutions was 829.6 mW cm^{-2} for the Xenon light source as measured by a light intensity meter (HSX-F500). The general visible light source was emitted by a 30 W Xenon lamp (NBeT Company, China), and the light intensity was detected to be 3.65 mW cm^{-2}. In addition, two 32 W low-pressure UV lamps (Cnlight Co. Ltd., Shanghai, China) with wavelengths of 254 nm and 185 nm, respectively were studied for comparison. The irradiation intensity of UV light at 254 nm wavelength was 3.7 mW cm^{-2} as measured by a UV intensity meter (ST-512). At regular time intervals, aliquots of the sample were taken using a syringe and filtered through a filter (Puradisc syringe filter, 0.2 µm, Whatman) before analysis. To avoid the possible impact of filter adsorption on PFOA concentration, the first 3 mL filtrate was discarded. All experiments were conducted in triplicate to ensure repeatability of results.

2.3. Catalyst characterization and analytical procedures

Powder X-ray diffraction (XRD) patterns were collected using a Bruker D8 Discover diffractometer using Cu Kα radiation, in the scattering angle 2θ range 0–80°. Catalyst

solutions were collected using a Shimadzu 1700 UV–Vis spectrophotometer operating in the wavelength range 200–800 nm. Zeta potential values were determined using a Nano-ZS Zeta-seizer (Malvern, Model: ZEN3600). Zeta potential was measured three times at each pH (50 scans each time), and the average and standard deviation were calculated.

A triple quadrupole ultra-high-performance liquid chromatography tandem mass spectrometer (UHPLC-MS/MS; LC/MS 8060, Shimadzu) equipped with a binary pump and Shim-pack column (1.6 μm, 2.0 mm × 50 mm) was used for the quantitative and qualitative analysis of PFOA and its degradation products (PFHpA, PFHxA, PFPeA, PFBA, PFPrA, TFA). The mobile phase A was Milli-Q water, and mobile phase B was methanol. The flow rate and injection volume were 0.40 mL min^{-1}, and 1 μL, respectively. The elution gradient of PFOA analysis method was initiated with 50% B for 2.5 min, then 100% B for the next 1 min, followed by 50% B for another 1.5 min. The total method run time was 5 min. The mass spectrometer was operated in multiple reaction monitoring (MRM) mode. For PFOA, mass to charge (*m/z)* ratios of 169.1 and 219.0 was used as the qualitative ions and *m/z* for the quantitation ion was 369.0 to avoid mass interference. The tandem mass spectrometry operating conditions of the target compounds are listed in **Table S1**.

3. Results and discussion

3.1. Characterization of catalysts

The XRD pattern of the commercial TiO_2 (P25) was exhibited in **Fig. S3** and the experimental XRD pattern agrees with the JCPDS card no. 21-1272 (anatase TiO_2) (Xu et al., 2015). The strong diffraction peaks at 25° and 48° confirmed the TiO_2 anatase structure and the broad diffraction peaks indicated very small size crystallite (Hussain et al., 2010). **Fig. S4** presented the UV-visible diffuse reflection absorption spectra of aqueous PFOA, PMS, TiO_2 and TiO_2/PMS. PFOA and PMS showed negligible absorbance for all the light resources. Comparatively, TiO_2 had the increasing absorbance ability of the light resource with the

decreasing light wavelength from 800 to 250 nm, which proved that TiO_2 had a certain ability for visible light absorption (400–800 nm) but which was worse than that for UV light (< 400 nm). However, when TiO_2 was mixed with PMS in the solution, promoted light absorbance was observed in the range of visible light resource (400–800 nm). This is probably because, in the mixed suspension, some visible-light absorbing complexes on TiO_2 surface were formed with the addition of PMS. Jo et al. (2018) investigated the activation of PMS with TiO_2 on visible light irradiation and claimed that surface charge-transfer complex (Ti-$OOSO_3^-$) was produced through the reaction (i.e. >TiO_2 + HSO_5^- → > Ti-$OOSO_3^-$ + H_2O), which was responsible for the visible light absorption in TiO_2/PMS suspensions.

3.2. Photocatalysis of PFOA

3.2.1. Degradation performance of PFOA under visible light

Comparative experiments with different catalysts (PMS, TiO_2, and TiO_2/PMS) of different amounts were conducted to explore the synergistic effect of TiO_2 and PMS under powerful visible light irradiation (300 W, 400-770 nm wavelength). For comparison, the same experiments were conducted under either darkness or general visible light (30 W). The initial concentration of PFOA was 50 mg L^{-1}, which was the level in some seriously contaminated water. The amount of PMS and TiO_2 used was set at 0.75 g L^{-1} and 0.25 g L^{-1}, respectively based on preliminary experiments, in either the separate system or the combined TiO_2/PMS system. In addition, different amounts of TiO_2 and PMS were used to create various TiO_2/PMS molar ratios, so as to probe the photodegradation mechanism. No other solution was added to adjust the pH value, and the initial pH of the solution was 3.0 ± 0.2.

As a result, **Fig. S5** shows that all the catalysts (i.e. PMS, TiO_2, and TiO_2/PMS) showed almost no catalytic ability for aqueous PFOA removal under either darkness or 30 W visible light, which indicates that PFOA could not be adsorbed by PMS or TiO_2 and these catalysts were not able to be activated under general visible light, respectively (Irie et al., 2003; Khan et al., 2017). Nevertheless, when the light source changed to a more powerful

visible light (300 W), the degradation performance was obviously promoted by PMS/TiO_2 that almost 100% of PFOA was degraded within 8 h. This was attributed to the fact that increasing the light intensity could active TiO_2 under visible light (400-700 nm) as eq. 1:

$$TiO_2 + hv \rightarrow h^+ + e^- \quad \text{(eq. 1)}$$

In theory, one photon energy (E_0) is calculated as: $E_0 = \frac{hc}{\lambda}$, where h is Planck's constant of 6.63×10^{-34} J·s, c is light speed of 3×10^8 m s^{-1}, λ is the wavelength of UV light, which is 400 nm, and thus E_0 was calculated to be 5.0×10^{-19} J. In addition, the band gap of TiO_2 is 3.14 eV or 5.0×10^{-19} J (1 eV = 1.6×10^{-19} J), which was approximately equal to E_0. Thus, visible light in general provided insufficient photons of high enough energy to active TiO_2 producing photogenerating hole and electron pairs. By increasing the light intensity to a certain level (300 W, 829.6 mW cm^{-2} in this study), TiO_2 could be activated as a photocatalyst under visible light. In previous studies, TiO_2 was modified with other materials to be utilized under visible light. For example, Sajid et al. (2016) reported that nitrogen-doped TiO_2 (N-doped TiO_2) exhibited broad absorption in the visible region, allowing the utilization of a large part of the solar spectrum for photocatalytic degradation of organic pollutants. Further investigation should focus on the N-doped TiO_2 with PMS under general visible light (about 30 W) or solar irradiation.

On the other hand, under powerful visible light, the degradation of PFOA by PMS alone was negligible, which means the sulfate radicals ($SO_4^{\bullet -}$), responsible for the PFOA degradation, may not be activated by visible light as shown in eq. 2 (Wang et al., 2015):

$$HSO_5^- + hv \rightarrow SO_4^{\bullet -} + \bullet OH \quad \text{(eq. 2)}$$

Comparably, sole TiO_2 showed only about 20% PFOA removal, while TiO_2/PMS generated the best catalytic performance for PFOA removal than sole PMS or TiO_2 as shown in **Fig. 1A**. The reason might be that holes and electrons could be generated on the surface of TiO_2

irradiated by powerful visible light as mentioned previous (Grilla et al., 2019), and HSO_5^- could react with photogenerated electron to form sulfate radicals ($SO_4^{\bullet-}$) as shown in eq. 3 (Shao et al., 2017). Thus, under powerful visible light, TiO_2/PMS outperformed than TiO_2 or PMS in degrading PFOA. Further reasons are discussed in section 3.3.

$$HSO_5^- + e^- \rightarrow SO_4^{\bullet-} + OH^- \qquad \text{(eq. 3)}$$

Also, the kinetics of the PFOA degradation fitted well to the pseudo-first-order model ($R^2 > 0.90$) described in eq. 4:

$$\ln (C_0/C_t) = k\,t \qquad \text{(eq. 4)}$$

where k is the rate constant (h^{-1}), C_0 and C_t (mg L^{-1}) are the concentrations of PFOA in the solution at irradiation time 0 and t (h), respectively. In the case of TiO_2/PMS, the rate constant was found to be 0.310 h^{-1}, which was almost 11 times higher than that of TiO_2 catalyst, which was only 0.028 h^{-1}. Nevertheless, until now, no previous study has been reported to achieve PFOA photocatalysis under visible light. Thus, the degradation of 50 mg L^{-1} aqueous PFOA within 8 h at the rate constant of 0.310 h^{-1} under 300 W visible light irradiation could be the reference of degradation efficiency for the future investigations on the PFOA photocatalysis under the similar external conditions of the study.

3.2.2. Effect of catalyst dosage

To select appropriate catalysts dosage, different amounts of PMS and TiO_2 were added in PFOA solution, PFOA removal in a photocatalysis process under 300 W visible light irradiation within 6 h is presented in **Fig. 1B**. When the dose of TiO_2 and PMS were 0.025 and 0.25 g L^{-1} with the ratio between them of 0.4:1, almost no PFOA was reduced by the photocatalysis. Because the low amount of TiO_2 could not provide sufficient active species such as photogenerated holes (h^+) and electrons (e^-) for PFOA degradation during the reaction process as eq. 2. However, increasing the molar ratio of TiO_2/PMS from 0.4:1 to 1.6:1, together with PMS constant of 0.25 g L^{-1} (namely [TiO_2] = 0.1 g L^{-1}, [PMS] = 0.25 g L^{-1}), the

degradation was increased to 34%. Further, the degradation of PFOA reached 48% when the molar ratio was increased to 3.9:1 (namely [TiO_2] = 0.25 g L^{-1}, [PMS] = 0.25 g L^{-1}). Thus, at 0.25 g L^{-1} PMS, increasing the ratio of TiO_2 could indeed improve the degradation effect. Also, when TiO_2 was kept to 0.25 g L^{-1}, but with the increase concentration of PMS from 0.25 to 0.75 g L^{-1} (the molar ratio of TiO_2/PMS decreased from 3.9:1 to 1.3:1), the degradation of PFOA increased obviously from 48% to 86%. Because the increasing ratio of PMS was able to produce more sulfate radicals (eq. 3), which has oxidative for the PFOA degradation. Nevertheless, when PMS concentration continually increased to 1.0 g L^{-1} (the ratio of TiO_2/PMS decreased to 1:1), the removal of PFOA did not increase further as expected. The reason could be explained that excessive sulfate radicals would react with each other to produce peroxydisulfate $\left(S_2O_8^{2-}\right)$ as shown in eq. 5:

$$SO_4^{\bullet-} + SO_4^{\bullet-} \rightarrow S_2O_8^{2-} \qquad \text{(eq. 5)}$$

Therefore, excessive ratio of PMS would instead inhibit the photodegradation process. Similarly, when PMS was kept as 0.75 g $L^{-1,}$ and TiO_2 concentration increased from 0.25 to 0.30 g L^{-1}, the degradation of PFOA slightly decreased from 86% to 73%. This might be attributed to that high concentration of TiO_2 would make the solution turbid, which reduced the photo permeability of visible light, leading to a negative effect on the degradation rate. Similar conclusion was also provided in the previous literatures (Aoudjit et al., 2019; Wang et al., 2014). Hence, on the treatment of 50 mg L^{-1} aqueous PFOA, the preferable amounts of catalyst were 0.25 g L^{-1} TiO_2 and 0.75 g L^{-1} PMS and the suitable molar ratio of TiO_2/PMS was 1.3:1.

3.2.3. Effect of solution pH

Fig. 2A shows the impact of initial pH (pH_0) on the catalytic performance for PFOA degradation in visible/TiO_2/PMS system. In detail, at pH_0 3 the degradation of PFOA was almost 100% under visible/TiO_2/PMS photodegradation for 8 h, which was the best

performance compared with the other pH conditions. With the increase of pH_0 to 5 and 7, within 8 h the degradation of PFOA was 90% and 45%, respectively. However, the removal of PFOA further dropped significantly to 24% at pH 9. In addition, the degradation rate increased with time and all followed the pseudo-first-order kinetic model under different pH_0 conditions. Moreover, the rate constant decreased with increase of initial solution pH in the order: k_{pH3} = 0.310 h^{-1} > k_{pH5} = 0.165 h^{-1} > k_{pH7} = 0.054 h^{-1} > k_{pH9} = 0.030 h^{-1}. Herein, the results indicated that the degradation efficacy of PFOA in visible/TiO_2/PMS was higher and faster when the solution pH was low.

Two reasons might explain such a phenomenon. First one was the reaction between the sulfate radical and OH^- ion to form hydroxyl radicals (•OH) as shown in eq. 6 (Liang, Wang & Bruell, 2007):

$$SO_4^{\bullet-} + OH^- \rightarrow SO_4^{2-} + \bullet OH \qquad \text{(eq. 6)}$$

Nevertheless, hydroxyl radicals have poor reactivity with PFOA, so the replacement of $SO_4^{\bullet-}$ by •OH would slow down the PFOA degradation (Hori et al., 2004; Lee et al., 2009).

The second reason is related to the Colombian attraction between the catalysts and pollutants. The surface zeta potential of TiO_2 (**Fig. S6**) continuously decreased with the increased of solution pH and the points of zero charge was 5.6. This means that when the solution pH was lower than 5.6, the surface of TiO_2 was positively charged in the form of ($TiOH_2^+$) due to the protonation (Xu et al., 2003), and negatively charged in the form of TiO^- in the solution when pH was above 5.6. On the other hand, the pK_a of PFOA is 2.8 (Goss, 2007). Therefore, when solution pH is more than 2.8, PFOA can get deprotonated form ($C_7F_{15}COO^-$) based on the reaction eq. 7:

$$C_7F_{15}COOH = H^+ + C_7F_{15}COO^- \qquad \text{(eq. 7)}$$

Thus, as shown in **Fig. S7**, when the solution pH was below 5.6 but over 2.8, PFOA could strongly interact with the TiO_2 by electrostatic interaction, leading to the accelerating

photodegradation efficacy. However, at pH 6 to 10, the surfaces of the catalysts were negatively charged due to the deprotonation (based on zeta potential value) resulting an electrostatic repulsion between PFOA (neutral or negatively charged PFOA) and the catalysts (negatively charged). Therefore, acidic condition (especially initial of pH 3 in this study) was the most beneficial for PFOA photodegradation in our system of visible/TiO_2/PMS.

3.2.4. Effect of light sources

The photocatalysis of aqueous PFOA was also evaluated by TiO_2/PMS under 32 W UV light with the two different wavelengths of 254 and 185 nm, compared with the performance in 300 W visible/TiO_2/PMS. Commonly, the UV light of 254 and 185 nm is frequently used in the study of photocatalysis process (Gomez-Ruiz et al., 2018; Xu et al., 2020). The 50 mg L^{-1} PFOA solution was treated by 0.5 g L^{-1} TiO_2 together with 0.15 g L^{-1} PMS without pH adjustment. As shown in **Fig. 2B**, the degradation efficiencies were almost similar for both wavelengths of 254 and 185 nm and their degradation were both almost 100% PFOA within 1.5 h. Thus, UV light irradiation significantly promoted the degradation rate as the reaction time was 8 h for 100% PFOA removal under 300 W visible light, which was more than 5 times longer than that under UV light. The reason might be related to the absorbance ability of different light resources by the catalysts. As shown in **Fig. S4**, the absorbance intensity was higher in UV wavelength (< 400 nm) than that in visible light wavelength (400-700 nm), and therefore more quantity of photons was absorbed in the system for the photodegradation. Also, the photon from UV light has higher energy than from visible light, which could irradiate more quantity of photoinduced hole and electron pairs, leading to a stronger redox ability for PFOA degradation. Such reasons were also discussed in previous research (Giri et al., 2012). Therefore, TiO_2/PMS have the stronger photocatalytic ability under UV light (both 254 and 185 nm UV light resources) than visible light, but may need more energy cost when considered the economy factor.

3.2.5. Advantages of photocatalysis by TiO_2/PMS

When compared with other materials in the previous studies (**Table 1**) (Li et al., 2016; Panchangam et al., 2009), the catalyst of TiO_2/PMS firstly investigated in this study presents excellent advantages on the treatment for aqueous PFOA. Initially, TiO_2/PMS utilized as catalyst under 300 W visible light irradiation could degrade PFOA from the solution and 100% PFOA was removal within 8 h. This finding provides the basic knowledge of solar application on the treatment of water containing PFAS with low secondary pollution. Secondly, TiO_2/PMS have comparatively high degradation ability under UV light irradiation compared with other findings as shown in **Table 1**. The fluence-based first-order rate constant (k_f, $cm^2\ mJ^{-1}$) and the half-life ($\tau_{1/2}$, h) were introduced to make a comprehensive comparison among different catalytic systems (Zhang et al., 2017). Notably, k_f of TiO_2/PMS under 254 nm UV light was $8.18 \times 10^{-4}\ cm^2\ mJ^{-1}$, higher than that of all the other catalysts except In_2O_3 PNPs under UV light. The $\tau_{1/2}$ value was found to increase as: $\tau_{1/2}$ (UV/In_2O_3 PNPs = 0.07 h) < $\tau_{1/2}$ (UV/β-Ga_2O_3 Nanorods = 0.27 h) < $\tau_{1/2}$ (UV/TiO_2/PMS = 0.64 h) < the other conditions. Finally, yet importantly, TiO_2/PMS was easy to be prepared by simply mixing the commercial TiO_2 and PMS powders in the solution. However, In_2O_3 PNPs and β-Ga_2O_3 Nanorod with shorter $\tau_{1/2}$ value need more complex synthesizing process than the preparation for TiO_2/PMS. For example, In_2O_3 porous nanoplates (PNPs) were synthesized by ethylenediamine-assisted hydrothermal process, which needs to be maintained at 180 °C for 16 h and 270 °C for 2 h in the air (Li et al., 2014). β-Ga_2O_3 Nanorods were obtained by microwave irradiation hydrothermal synthesis procedure from the precursor of $Ga(NO_3)_3 \cdot H_2O$ (Zhao et al., 2015). Overall, TiO_2/PMS should be considered as the potential catalyst applied for the photocatalysis of PFOA no matter under visible light (300 W) for energy saving or UV light for the high degradation efficiency.

3.3. Proposed degradation mechanism

3.3.1. Intermediates analysis

The intermediates such as PFHpA, PFHxA, PFPeA, PFBA, PFPA and TFA during PFOA photocatalytic process in visible/TiO_2/PMS system were identified and quantified by UHPLC-MS/MS as shown in **Fig. S8**. The *m/z* ratio of individual compound and the other MS/MS parameters were listed in **Table S1**. Thereupon, the time dependence of PFOA and these intermediates were described in **Fig. 3A**. Clearly, PFHpA was first produced, and its concentration was increased to the maximum of 0.5 mg L^{-1} within 6 h and then decreased. PFHxA was initially detected after 2 h and continuously increased to 1.0 mg L^{-1} within 8 h. PFPeA increased during the time from 4 to 8 h reaction course. However, the concentrations of shorter chain compounds such as PFBA PFPA and TFA were below the limit of quantification. The findings indicate that the photocatalytic process of PFOA proceeds in a step-by-step fashion from PFOA to shorter chain intermediates (i.e. PFHpA, PFHxA, and PFPeA) as reported in the literature (Li et al., 2016; Li et al., 2012; Wu et al., 2018).

3.3.2. Active species analysis

During the photocatalytic process in visible/TiO_2/PMS system, four types of active species, including photoinduced holes (h^+) and electrons (e^-), hydroxyl radical (•OH), sulfate radicals ($SO_4^{\bullet-}$) and superoxide radical ($O_2^{\bullet-}$) are supposed to be generated as shown in eqs 2, 8 and 9, which own the oxidative and reduction ability contributing the PFOA degradation.

$$TiO_2\ (h^+) + H_2O \rightarrow TiO_2 + \bullet OH + H^+ \qquad \text{(eq. 8)}$$

$$TiO_2\ (e^-) + O_2 \rightarrow O_2^{\bullet-} \qquad \text{(eq. 9)}$$

To prove the degradation ability of these four species, tertbutanol (t-BuOH), disodium ethylenediaminetetraacetate (EDTA-Na_2) and benzoquinone (BQ) were added into the system, which was used as scavengers of •OH, holes and $O_2^{\bullet-}$, respectively. Degradation by TiO_2 only was used to simulate the condition of adding the scavenger of $SO_4^{\bullet-}$ radicals. As shown in **Fig. 3B**, it is easily observed that degradation by only TiO_2 has the poorest

photodegradation performance that only 20% PFOA was removal within 8 h, which proves that $SO_4^{\bullet-}$ radicals play the essential roles in visible/TiO_2/PMS system for PFOA degradation. Secondly, the addition of EDTA-Na_2 in the reaction solution caused only 40% PFOA removal, which indicates that the photoinduced holes, rather than electrons, could largely react with the absorbed PFOA molecules directly and played the main role in degrading PFOA in the photocatalytic system. While the scavengers of BQ and *t*-BuOH have less negative effect for the degradation efficacy compared with the others. When BQ was added, 63% PFOA was degraded, which suggests that PFOA photodegradation was less influenced by $O_2^{\bullet-}$ radicals generated. Furthermore, when *t*-BuOH was added in the system, 77% PFOA removal was observed on the degradation rate. This suggests that that hydroxyl radical (•OH) owns the worst degradation ability for PFOA than the other species, and it is consistent with the theory that •OH has poor reactivity with PFOA as mentioned in the section 3.2.3. On the other hand, based on degradation curves of different scavengers within 6 h photocatalysis, the rate constant ranked from highest to lowest was as follows: $k_{(\text{No addition})} = 0.310\ h^{-1} > k_{(\text{t-BuOH})} = 0.154\ h^{-1} > k_{(\text{BQ})} = 0.112\ h^{-1} > k_{(\text{EDTA-Na2})} = 0.058\ h^{-1} > k_{(\text{Only TiO2})} = 0.028\ h^{-1}$. Thus, it means that the active species produced during the photocatalytic process from most important to least for PFOA degrading was followed by: $SO_4^{\bullet-}$ radicals > photoinduced holes (h^+) > $O_2^{\bullet-}$ radicals > •OH. Besides, in the visible/TiO_2/PMS system, photoinduced holes (h^+) rather than electrons (e^-) played the main role in PFOA degradation.

3.3.3. Possible degradation pathway

Based on the intermediates and active species analysis during the photocatalytic process, the primary degradation mechanism occurring in visible/TiO_2/PMS would be proposed as the following equations (10-18):

Part of PFOA in the solution could exist as an anionic compound ($C_7F_{15}COO^-$) and was absorbed on the surface of TiO_2 (Chen et al., 2015):

$$C_7F_{15}COOH + H_2O \rightarrow C_7F_{15}COO^- + H_3O^+ \quad \text{(eq. 10)}$$

Then, $C_7F_{15}COO^-$ reacts with sulfate radicals $\left(SO_4^{\bullet -}\right)$ or photoinduced holes (h^+) to form perfluoroperoxy radicals ($C_7F_{15}COO\bullet$) (Wu et al., 2016).

$$C_7F_{15}COO^- + SO_4^{\bullet -} \rightarrow C_7F_{15}COO\bullet + SO_4^{2-} \quad \text{(eq. 11)}$$

$$C_7F_{15}COO^- + h^+ \rightarrow C_7F_{15}COO\bullet \quad \text{(eq. 12)}$$

While the $C_7F_{15}COO\bullet$ is quite unstable and then spontaneously undergo Kolbe decarboxylation to form $C_7F_{15}\bullet$ radicals (Chen et al., 2015).

$$C_7F_{15}COO\bullet \rightarrow C_7F_{15}\bullet + CO_2\uparrow \quad \text{(eq. 13)}$$

Then formed $C_7F_{15}\bullet$ react with water to form $C_6F_{13}COF$ after H+ and F^- elimination (Nohara et al., 2001):

$$C_7F_{15}\bullet + H_2O \rightarrow C_7F_{15}OH + H^+ \quad \text{(eq. 14)}$$

$$C_7F_{15}OH \rightarrow C_6F_{13}COF + HF \quad \text{(eq. 15)}$$

By hydrolysis, $C_6F_{13}COF$ is converted into PFHpA ($C_6F_{13}COOH$) with F^- reduced (Hori et al., 2008).

$$C_6F_{13}COF + H_2O \rightarrow C_6F_{13}COOH\ (PFHpA) + HF \quad \text{(eq. 16)}$$

Furthermore, PFHpA was decomposed into PFHxA, and PFPeA proved in this study, and would continually change to PFBA, PFPA and TPA in the same way and finally mineralized to CO_2 and fluoride ions in the stepwise manner as reported by previous literatures (Jiang et al., 2016; Liu et al., 2019).

Consequently, the excellence synergistic effect between TiO_2 and PMS for PFOA removal was attributed to that both sulfate radicals (produced by PMS) and photoinduced holes (produced by TiO_2) had the strong photocatalytic ability for PFOA degradation (as shown in eqs 11 and 12). Besides, photoinduced electrons (e^-) could both reacted with PMS (HSO_5^-) and peroxydisulfate $\left(S_2O_8^{2-}\right)$ to form sulfate radicals (as shown in eqs 3 and 17), which not only increased the quantity of sulfate radicals in the solution but also inhibited the

recombination of photoinduced holes and electrons (eq.18) as the electrons were consumed in the reaction of eq.3 and 17. Thus, the amount of photoinduced holes and sulfate radicals was primarily increased during the photocatalytic reaction in visible/TiO_2/PMS, leading to a higher degradation efficiency than that in sole PMS or TiO_2 system.

$$S_2O_8^{2-} + e^- \rightarrow SO_4^{\bullet -} \quad \text{(eq. 17)}$$

$$h^+ + e^- \rightarrow \text{recombination} \quad \text{(eq. 18)}$$

Besides, as shown in **Fig. S4**, TiO_2/PMS have higher visible light absorbance than TiO_2 and PMS, which also contributes to the fact that visible/TiO_2/PMS outperformed visible/TiO_2 and visible/PMS in PFOA photocatalysis degradation.

3.4. Photocatalysis application in wastewater

The photocatalyst TiO_2 has been widely used nowadays in many applications such as enhancing the photocatalytic property or development of new photocatalytic thin films (Ghori et al., 2018; Yu et al., 2018). In this study, to validate the feasibility of TiO_2/PMS photocatalysis to degrade PFOA in the real wastewater, as the coexisting compounds may reduce the degradation efficacy (Beltran et al., 2008), the photodegradation of PFOA in the influent and effluent samples taken from a municipal sewage treatment plant in Sydney, Australia was investigated. The characteristics of these wastewater samples are listed in **Table 2**. The original pH of wastewater samples was 6.15 to 6.17. When PFOA and the catalysts of TiO_2/PMS were introduced, the pH of the suspension was changed to 3.0 ± 0.2 without pH adjustment. Herein, 50 mg L^{-1} PFOA in the influent and effluent samples were dosed with 0.25 g L^{-1} TiO_2 and 0.75 g L^{-1} PMS for the photocatalysis under 300 W visible light, 254 and 185 nm UV light irradiation, respectively. As a result, **Fig. 4A** shows that in the powerful visible light system, 65-82% PFOA was degraded within 8 h by TiO_2/PMS in influent and effluent samples and their rate constant was 0.136 and 0.070 h^{-1}, respectively, which were both lower than that in pure water (k = 0.310 h^{-1}). The reduction in rate constant was probably due to the adverse impacts of coexisting organic matter in these sewage water

samples, leading to the reduced performance for PFOA removal (Shao et al., 2013). However, in the UV light system, the photodegradation performance in the wastewater was as effective as in pure water, reflecting the stable photocatalytic ability of TiO_2/PMS under UV light irradiation (both in 254 and 185 nm), which was not easily disturbed by other organic compounds in the real wastewater samples.

Total organic carbon (TOC) was another important index reflecting the degradation effect, so the changes of TOC with time were also measured in this study. As it can be deduced from **Fig. 4B**, in the influent sample, 65% TOC was removed in 254 nm UV/TiO_2/PMS system, whereas 34% TOC was removed in 185 nm UV/TiO_2/PMS system and 26% TOC was removed in 300 W visible/TiO_2/PMS system. Similarly, in the effluent sample, the rate of TOC removal was reduced as: 254-nm UV/TiO_2/PMS (69%) > 185-nm UV/TiO_2/PMS (53%) > 300 W visible/TiO_2/PMS (44%). Because 254 nm UV light is fairly well transmitted as water molecules do not absorb the energy corresponding to this wavelength, while 185 nm intensity drops as it is absorbed by water molecules (Imoberdorf and Mohseni, 2011). Thus, although 185 nm UV light is more powerful than 254 nm, it is does not transmit as well through water as 254 nm, leading to the various degradation performance between TOC and PFOA removal in the real wastewater.

4. Conclusions

In summary, the visible/TiO_2/PMS system could degrade 100% of PFOA at 50 mg L^{-1} within 8 h, which was better than sole PMS or TiO_2 under the same conditions. Based on extensive experiments considering influencing factors, a combination of 0.25 g L^{-1} TiO_2 and 0.75 g L^{-1} PMS in the reaction solution with the initial pH 3 generated the best performance than under the other conditions in this study. Furthermore, under UV light irradiation at 254 and 185 nm wavelengths, TiO_2/PMS both achieved excellent degradation efficacy of PFOA (almost 100%) within 1.5 h. According to the analysis of intermediates, PFOA was gradually

decomposed from the long chain into shorter chain species during the photocatalytic process. Scavenger experiments proved that $SO_4^{\bullet-}$ radicals and photogenerated holes were the most important active species contributing to the PFOA photodegradation. In real wastewater samples, 65-82% PFOA degradation and 26-44% TOC removal were achieved after the treatment by TiO_2/PMS under 300 W visible light irradiation. Overall, the TiO_2/PMS system under powerful visible light can potentially be applied for PFAS photocatalysis in water and wastewater.

Acknowledgements

The authors would like to thank the China Scholarship Council (CSC) and the University of Technology Sydney for financial support (Grant No. 201606890028).

References

Aoudjit, F., Cherifi, O., Halliche, D., 2019. Simultaneously efficient adsorption and photocatalytic degradation of sodium dodecyl sulfate surfactant by one-pot synthesized TiO_2/layered double hydroxide materials. Sep. Sci. Technol. 54, 1095-1105.

Bassler, J., Ducatman, A., Elliott, M., Wen, S., Wahlang, B., Barnett, J., Cave, M.C., 2019. Environmental perfluoroalkyl acid exposures are associated with liver disease characterized by apoptosis and altered serum adipocytokines. Environ. Pollut. 247, 1055-1063.

Behr, A.C., Lichtenstein, D., Braeuning, A., Lampen, A., Buhrke, T., 2018. Perfluoroalkylated substances (PFAS) affect neither estrogen and androgen receptor activity nor steroidogenesis in human cells in vitro. Toxicol. Lett. 291, 51-60.

Beltran, F.J., Aguinaco, A., Garcia-Araya, J.F, Oropesa, A., 2008. Ozone and photocatalytic processes to remove the antibiotic sulfamethoxazole from water. Water Res. 42, 3799-3808.

Cao, Y., Li, Q., Li, C., Li, J., Yang, J., 2016. Surface heterojunction between (001) and (101) facets of ultrafine anatase TiO_2 nanocrystals for highly efficient photoreduction CO_2 to CH_4. Appl. Catal. B 198, 378-388.

Chen, M.J., Lo, S.L., Lee, Y.C., Huang, C.C., 2015. Photocatalytic decomposition of perfluorooctanoic acid by transition-metal modified titanium dioxide. J. Hazard. Mater. 288, 168-175.

Chen, X., Wang, W., Xiao, H., Hong, C., Zhu, F., Yao, Y., Xue, Z., 2012. Accelerated TiO_2 photocatalytic degradation of Acid Orange 7 under visible light mediated by peroxymonosulfate. Chem. Eng. J. 193-194, 290-295.

Feng, Y., Liao, C., Kong, L., Wu, D., Liu, Y., Lee, P.H., Shih, K., 2018. Facile synthesis of highly reactive and stable Fe-doped g-C_3N_4 composites for peroxymonosulfate activation: A novel nonradical oxidation process. J. Hazard. Mater. 354, 63-71.

Gao, L., Minakata, D., Wei, Z., Spinney, R., Dionysiou, D.D., Tang, C.J., Chai, L., Xiao, R., 2018. Mechanistic study on the role of soluble microbial products in sulfate radical-mediated degradation of pharmaceuticals. Environ. Sci. Technol. 53, 342-353.

Ghori, M.Z., Veziroglu, S., Henkel, B., Vahl, A., Polonskyi, O., Strunskus, T., Faupel, F., Aktas, O.C., 2018. A comparative study of photocatalysis on highly active columnar TiO_2 nanostructures in-air and in-solution. Sol. Energy Mater. Sol. Cells 178, 170-178.

Giri, R.R., Ozaki, H., Okada, T., Taniguchi, S., Takanami, R., 2012. Factors influencing UV photodecomposition of perfluorooctanoic acid in water. Chem. Eng. J. 180, 197-203.

Gomez-Ruiz, B., Ribao, P., Diban, N., Rivero, M.J., Ortiz, I., Urtiaga, A., 2018. Photocatalytic degradation and mineralization of perfluorooctanoic acid (PFOA) using a composite TiO_2−rGO catalyst. J. Hazard. Mater. 344, 950-957.

Goss, K.U., 2007. The pK_a values of PFOA and other highly fluorinated carboxylic acids. Environ. Sci. Technol. 42, 456-458.

Grilla, E., Matthaiou, V., Frontistis, Z., Oller, I., Polo, I., Malato, S., Mantzavinos, D., 2019. Degradation of antibiotic trimethoprim by the combined action of sunlight, TiO_2 and persulfate: A pilot plant study. Catal. Today 328, 216-222.

Hao, Q., Liu, Y., Chen, T., Guo, Q., Wei, W., Ni, B.J., 2019. Bi_2O_3@ Carbon nanocomposites for solar-driven photocatalytic degradation of chlorophenols. ACS Appl. Nano Mater. 2, 2308-2316.

Hori, H., Hayakawa, E., Einaga, H., Kutsuna, S., Koike, K., Ibusuki, T., Kiatagawa, H., Arakawa, R., 2004. Decomposition of environmentally persistent perfluorooctanoic acid in water by photochemical approaches. Environ. Sci. Technol. 38, 6118-6124.

Hori, H., Yamamoto, A., Koike, K., Kutsuna, S., Murayama, M., Yoshimoto, A., Arakawa, R., 2008. Photocatalytic decomposition of a perfluoroether carboxylic acid by tungstic heteropolyacids in water, Appl. Catal. B 82, 58-66.

Hurley, S., Goldberg, D., Wang, M., Park, J.S., Petreas, M., Bernstein, L., Anton-Culver, H., Nelson, D.O., Reynolds, P., 2018. Breast cancer risk and serum levels of per-and poly-fluoroalkyl substances: a case-control study nested in the California Teachers Study. Environ. Health 17, 83.

Hussain, M., Ceccarelli, R., Marchisio, D.L., Fino, D., Russo, N., Geobaldo, F., 2010. Synthesis, characterization, and photocatalytic application of novel TiO_2 nanoparticles. Chem. Eng. J. 157, 45-51.

Imoberdorf, G., Mohseni, M., 2011. Degradation of natural organic matter in surface water using vacuum-UV irradiation. J. Hazard. Mater. 186, 240-246.

Irie, H., Watanabe, Y., Hashimoto, K., 2003. Carbon-doped anatase TiO_2 powders as a visible-light sensitive photocatalyst. Chem. Lett. 32 (8), 772-773.

Janousek, R.M., Mayer, J., Knepper, T.P., 2019. Is the phase-out of long-chain PFASs measurable as fingerprint in a defined area? Comparison of global PFAS concentrations and a monitoring study performed in Hessen, Germany from 2014-2018. TrAC Trends Anal. Chem. https://doi.org/10.1016/j.trac.2019.01.017.

Jiang, F., Zhao, H., Chen, H., Xu, C., Chen, J., 2016. Enhancement of photocatalytic decomposition of perfluorooctanoic acid on CeO_2/In_2O_3. RSC Adv. 6, 72015-72021.

Jo, Y., Kim, C., Moon, G.-H., Lee, J., An, T., Choi, W., 2018, Activation of peroxymonosulfate on visible light irradiated TiO2 via a charge transfer complex path. Chem. Eng. J. 346, 249-257.

Khan, S., Han, C., Khan, H.M., Boccelli, D.L., Nadagouda, M.N., Dionysiou, D.D., 2017. Efficient degradation of lindane by visible and simulated solar light-assisted S-TiO_2/peroxymonosulfate process: Kinetics and mechanistic investigations. Mol. Catal. 428, 9-16.

Lee, Y.C., Lo, S.L., Chiueh, P.T., Chang, D.G., 2009. Efficient decomposition of perfluorocarboxylic acids in aqueous solution using microwave-induced persulfate. Water Res. 43, 2811-2816.

Li, M., Yu, Z., Liu, Q., Sun, L., Huang, W., 2016. Photocatalytic decomposition of perfluorooctanoic acid by noble metallic nanoparticles modified TiO_2. Chem. Eng. J. 286, 232-238.

Li, Z., Zhang, P., Li, J., Shao, T., Wang, J., Jin, L., 2014. Synthesis of In_2O_3 porous nanoplates for photocatalytic decomposition of perfluorooctanoic acid (PFOA). Catal. Commun. 43, 42-46.

574 Li, Z., Zhang, P., Shao, T., Li, X., 2012. In_2O_3 nanoporous nanosphere: A highly efficient
575 photocatalyst for decomposition of perfluorooctanoic acid. Appl. Catal. B 125, 350-
576 357.
577 Liang, C., Wang, Z.S., Bruell, C.J., 2007, Influence of pH on persulfate oxidation of TCE at
578 ambient temperatures. Chemosphere 66, 106-113.
579 Liu, Y., Fan, X., Quan, X., Fan, Y., Chen, S., Zhao, X., 2019. Enhanced perfluorooctanoic
580 acid degradation by electrochemical activation of sulfate solution on B/N codoped
581 diamond. Environ. Sci. Technol. 53, 5195-5201.
582 Liu, Z., Lu, Y., Wang, T., Wang, P., Li, Q., Johnson, A.C., Sarvajayakesavalu, S., Sweetman,
583 A.J., 2016. Risk assessment and source identification of perfluoroalkyl acids in
584 surface and ground water: Spatial distribution around a mega-fluorochemical
585 industrial park, China. Environ. Int. 91, 69-77.
586 Nohara, K., Toma, M., Kutsuna, S., Takeuchi, K., Ibusuki, T., 2001. Cl atom-initiated
587 oxidation of three homologous methyl perfluoroalkyl ethers. Environ. Sci. Technol.
588 35, 114-120.
589 Pan, M., Huang, N., Zhao, X., Fu, J., Zhong, X., 2013. Enhanced efficiency of dye-sensitized
590 solar cell by high surface area anatase-TiO_2-modified P25 paste. J. Nanomater. 2013,
591 760685.
592 Panchangam, S.C., Lin, A.Y., Shaik, K.L., Lin, C.F., 2009. Decomposition of
593 perfluorocarboxylic acids (PFCAs) by heterogeneous photocatalysis in acidic aqueous
594 medium. Chemosphere 77, 242-248.
595 Park, K., Ali, I., Kim, J.O., 2018. Photodegradation of perfluorooctanoic acid by graphene
596 oxide-deposited TiO_2 nanotube arrays in aqueous phase. J. Environ. Manage. 218,
597 333-339.
598 Shao, H., Zhao, X., Wang, Y., Mao, R., Wang, Y., Qiao, M., Zhao, S., Zhu, Y. 2017.
599 Synergetic activation of peroxymonosulfate by Co_3O_4 modified g-C_3N_4 for enhanced

degradation of diclofenac sodium under visible light irradiation. Appl. Catal. B 218, 810-818.

Shao, T., Zhang, P., Jin, L., Li, Z., 2013. Photocatalytic decomposition of perfluorooctanoic acid in pure water and sewage water by nanostructured gallium oxide. Appl. Catal. B 142-143, 654-661.

Sornalingam, K., McDonagh, A., Zhou, J.L., 2016. Photodegradation of estrogenic endocrine disrupting steroidal hormones in aqueous systems: progress and future challenges. Sci. Total Environ. 550, 209-224

Valsecchi, S., Rusconi, M., Mazzoni, M., Viviano, G., Pagnotta, R., Zaghi, C., Serrini, G., Polesello, S., 2015. Occurrence and sources of perfluoroalkyl acids in Italian river basins. Chemosphere 129, 126-134.

Wang, X., Wu, P., Lu, Y., Huang, Z., Zhu, N., Lin, C., Dang, Z., 2014. NiZnAl layered double hydroxides as photocatalyst under solar radiation for photocatalytic degradation of orange G. Sep. Purif. Technol. 132, 195-205.

Wang, Y., Zhang, P., 2011. Photocatalytic decomposition of perfluorooctanoic acid (PFOA) by TiO_2 in the presence of oxalic acid. J. Hazard. Mater. 192, 1869-1875.

Wang, Y., Zhou, L., Duan, X., Sun, H., Tin, E.L., Jin, W., Wang, S., 2015. Photochemical degradation of phenol solutions on Co_3O_4 nanorods with sulfate radicals. Catal. Today 258, 576-584.

Wu, D., Li, X., Zhang, J., Chen, W., Lu, P., Tang, Y., Li, L., 2018. Efficient PFOA degradation by persulfate-assisted photocatalytic ozonation. Sep. Purif. Technol. 207, 255-261.

Wu, Y., Li, Y., Tian, A., Mao, K., Liu, J., 2016. Selective removal of perfluorooctanoic acid using molecularly imprinted polymer-modified TiO_2 nanotube arrays. Int. J. Photoenergy 2016, 7368795.

Xiao, R., Gao, L., Wei, Z., Spinney, R., Luo, S., Wang, D., Dionysiou, D.D., Tang, C.J., Yang, W., 2017. Mechanistic insight into degradation of endocrine disrupting chemical by hydroxyl radical: an experimental and theoretical approach. Environ. Pollut. 231, 1446-1452.

Xu, B., Ahmed, M.B., Zhou, J.L., Altaee, A., Wu, M., Xu, G., 2017. Photocatalytic removal of perfluoroalkyl substances from water and wastewater: Mechanism, kinetics and controlling factors. Chemosphere 189, 717-729.

Xu, B., Ahmed, M.B., Zhou, J.L., Altaee, A., Xu, G., Wu, M., 2018. Graphitic carbon nitride based nanocomposites for the photocatalysis of organic contaminants under visible irradiation: Progress, limitations and future directions. Sci. Total Environ. 633, 546-559.

Xu, B., Zhou, J.L., Altaee, A., Ahmed, M.B., Johir, M.B., Ren, J., Li, X., 2020. Improved photocatalysis of perfluorooctanoic acid in water and wastewater by Ga_2O_3/UV system assisted by peroxymonosulfate. Chemosphere 239, 124722.

Xu, G., Zhang, J., Li, G., Song, G., 2003. Effect of complexation on the zeta potential of titanium dioxide dispersions. J. Dispersion Sci. Technol. 24, 527-535.

Xu, H., Li, G., Zhu, G., Zhu, K., Jin, S., 2015. Enhanced photocatalytic degradation of rutile/anatase TiO_2 heterojunction nanoflowers. Catal. Commun. 62, 52-56.

Yoo, J., Zazpe, R., Cha, G., Prikryl, J., Hwang, I., Macak, J.M., Schmuki, P., 2018. Uniform ALD deposition of Pt nanoparticles within 1D anodic TiO_2 nanotubes for photocatalytic H_2 generation. Electrochem. Commun. 86, 6-11.

Yu, X., Ren, N., Qiu, J., Sun, D., Li, L., Liu, H., 2018. Killing two birds with one stone: To eliminate the toxicity and enhance the photocatalytic property of CdS nanobelts by assembling ultrafine TiO_2 nanowires on them. Sol. Energy Mater. Sol. Cells 183, 41-47.

650 Zhang, Y., Liu, X., Li, P., Duan, Y., Hu, X., Li, F., Song, Y., 2019. Dopamine-crosslinked
651 TiO_2/perovskite layer for efficient and photostable perovskite solar cells under full
652 spectral continuous illumination. Nano Energy 56, 733-740.
653 Zhang, Y., Zhang, J., Xiao, Y., Chang, V.W., Lim, T.T., 2017. Direct and indirect
654 photodegradation pathways of cytostatic drugs under UV germicidal irradiation:
655 process kinetics and influences of water matrix species and oxidant dosing. J. Hazard.
656 Mater. 324, 481-488.
657 Zhao, B., Li, X., Yang, L., Wang, F., Li, J., Xia, W., Li, W., Zhou, L., Zhao, C., 2015. β-
658 Ga_2O_3 nanorod synthesis with a one-step microwave irradiation hydrothermal method
659 and its efficient photocatalytic degradation for perfluorooctanoic acid. Photochem.
660 Photobiol. 91, 42-47.

Table 1

Comparison of photocatalytic conditions for PFOA removal by TiO_2/PMS and other catalysts.

Catalyst	Catalyst dosage ($g\ L^{-1}$)	Light source	Light intensity ($mW\ cm^{-2}$)	C_0 (PFOA) ($mg\ L^{-1}$)	Removal (reaction period)	k_t (h^{-1})	[a]k_f ($cm^2\ mJ^{-1}$)	[b]$\tau_{1/2}$ (h)	Reference
TiO_2/PMS	0.25/0.75	300 W, λ=400–770 nm	829.6	50	100% (8 h)	0.310	1.04×10^{-7}	2.24	This study
TiO_2/PMS	0.25/0.75	32 W, λ=254 nm	3.7	50	98% (1.5 h)	1.09	8.18×10^{-4}	0.64	This study
TiO_2 with $HClO_4$	0.7	16 W, λ=254 nm	0.45	50	86% (7 h)	0.282	1.74×10^{-4}	2.46	Panchangam et al., 2009a
TiO_2 with Pt	0.5	125 W, λ=365 nm	5.3	60	100% (5 h)	0.726	0.38×10^{-4}	0.95	Li et al., 2016b
TiO_2 with Pd	0.5	125 W, λ=365 nm	5.3	60	98% (7 h)	0.438	0.23×10^{-4}	1.58	Li et al., 2016b
TiO_2 with Ag	0.5	125 W, λ=365 nm	5.3	60	45% (7 h)	0.126	0.07×10^{-4}	5.50	Li et al., 2016b
β-Ga_2O_3 Nanorod	0.5	50 W, λ=254 nm	35	10	100% (1.5 h)	2.58	0.20×10^{-4}	0.27	Zhao et al., 2015
In_2O_3 PNPs	0.5	15 W, λ=254 nm	3.2	30	100% (0.5 h)	9.48	8.23×10^{-4}	0.07	Li et al., 2014

[a]The fluence-based first-order rate constant k_f ($cm^2\ mJ^{-1}$) is calculated as follows: $k_f = \frac{k_t}{I}$, where I is the light intensity.

[b]The half-life ($\tau_{1/2}$) of the reactants is described as: $\tau_{1/2} = \frac{In2}{k_t}$.

Table 2

Characteristics of the influent and effluent from a municipal wastewater plant in Sydney, Australia.

Effluent		Influent	
Parameter	Value	Parameter	value
PFOA	<LOQ[a]	PFOA	<LOQ[a]
TOC	14.41 mg L^{-1}	TOC	10.64 mg L^{-1}
TDS	659 mg L^{-1}	TDS	693 mg L^{-1}
$N\text{-}NH_4^+$	1.0 mg L^{-1}	$N\text{-}NH_4^+$	0.7 mg L^{-1}
$P\text{-}PO_4^{3-}$	6.7 mg L^{-1}	$P\text{-}PO_4^{3-}$	6.8 mg L^{-1}
pH	6.17	pH	6.15

[a] Limit of quantification

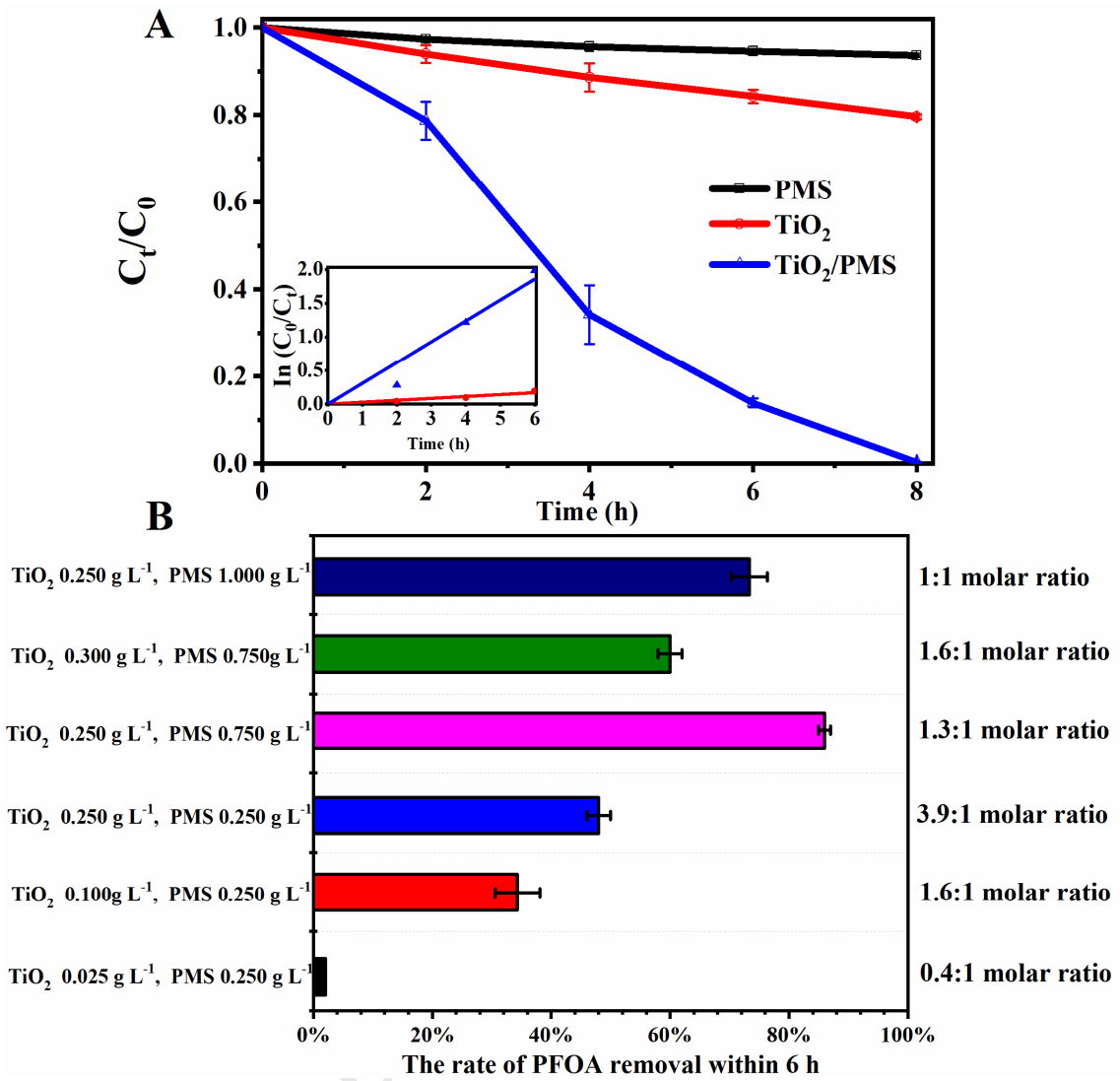

Fig. 1. (A) Degradation rate of PFOA (50 mg L^{-1}) in the system of PMS (0.75 g L^{-1}), TiO_2 (0.25 g L^{-1}) and TiO_2/PMS (0.25 g L^{-1}/0.75 g L^{-1}), respectively under 300-W visible light irradiation. Enlarged view of degradation curves within 6 h and the histogram of each degradation rate constant (*k*) was also provided. (B) Degradation rate of 50 mg L^{-1} PFOA by different amount of TiO_2/PMS under visible light.

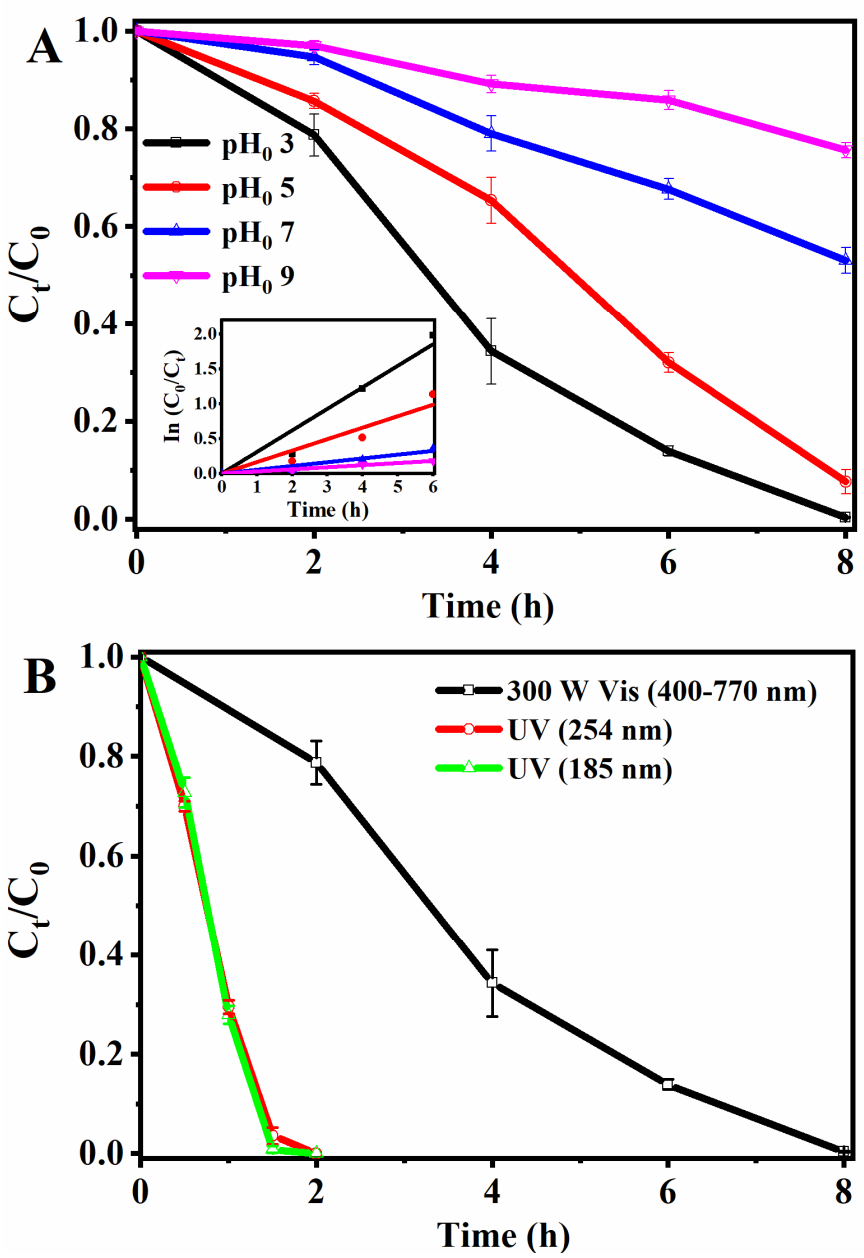

Fig. 2. (A) Effect of different initial solution pH (3, 5, 7 and 9) on PFOA degradation in visible/TiO_2/PMS system. Insert showing the fitting of degradation curves within 6 h and degradation rate constant (*k*) derived. (B) Effect of different light source on PFOA degradation by TiO_2/PMS. Visible light (300 W, 400-770 nm) was produced by a Xenon lamp, and 254 nm and 185 nm UV light were from two types of low-pressure UV lamps, respectively ([PFOA] = 50 mg L^{-1}, [PMS] 0.75 g L^{-1}, and [TiO_2] = 0.25 g L^{-1}).

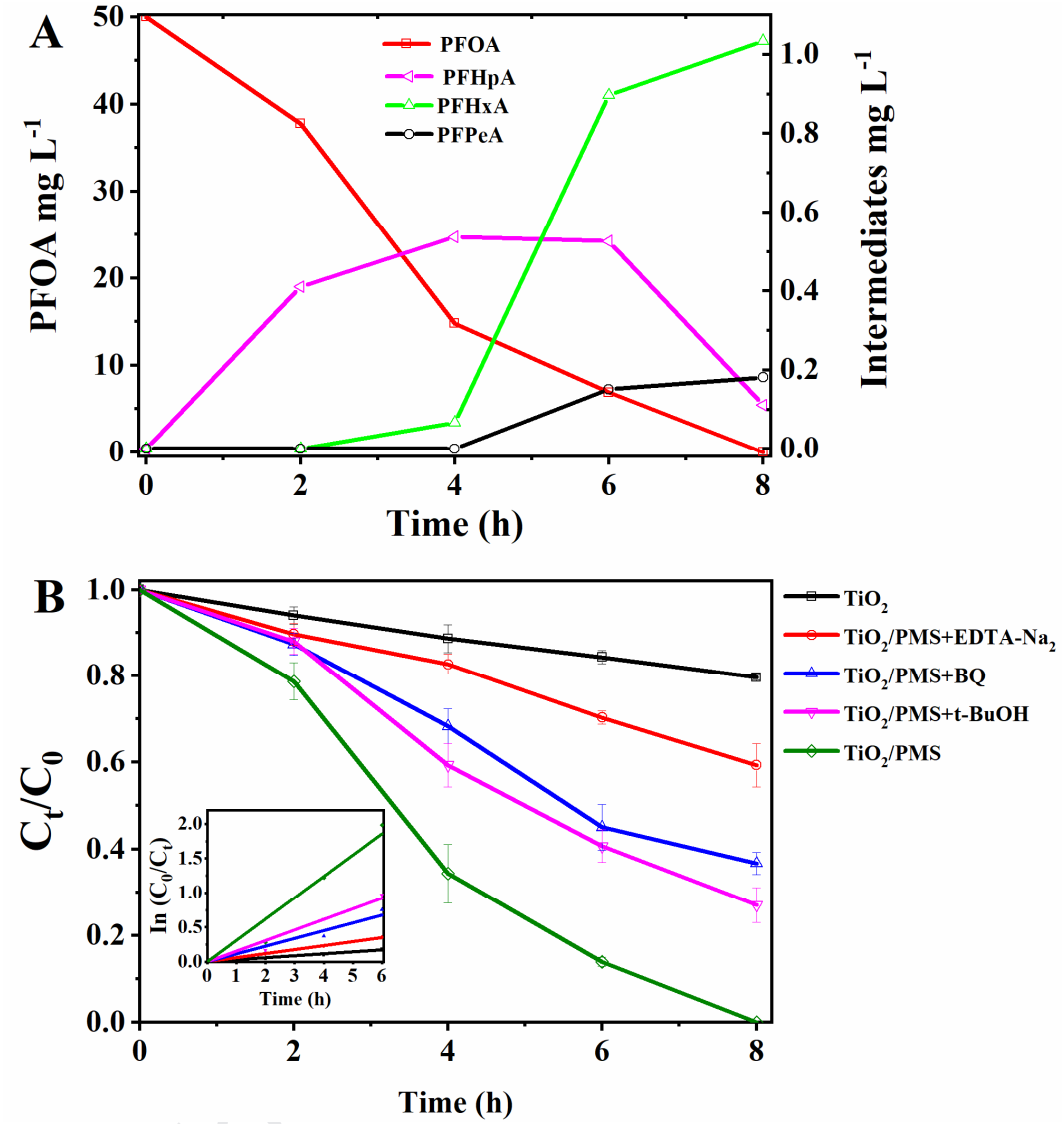

Fig. 3. (A) Time dependence of PFOA and its shorter-chain PFAS intermediates. (B) Effects of different scavengers (i.e. pure TiO_2, EDTA-Na_2, BQ, *t*-BuOH, and no scavengers) on the PFOA degradation in visible/TiO_2/PMS system within 8 h (300 W visible light, [PFOA] = 50 mg L^{-1}, [PMS] = 0.15 g L^{-1}, [TiO_2] = 0.05 g L^{-1}). Insert showing the fitting of degradation curves within 6 h and degradation rate constant (*k*) derived.

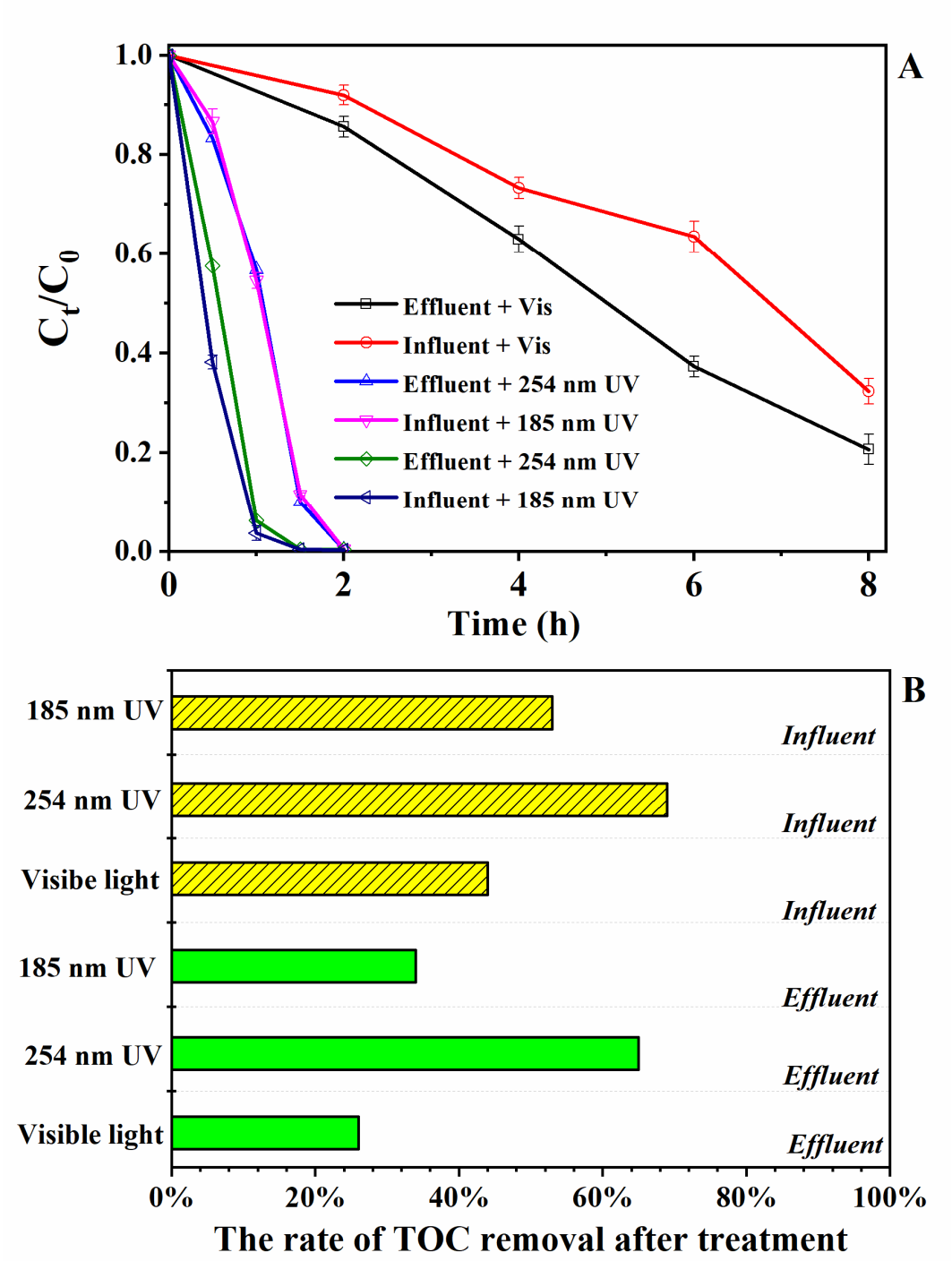

Fig. 4. (A) Degradation of PFOA in wastewater samples including influent and effluent from a wastewater treatment plant, and (B) rate of TOC removal by TiO_2/PMS under 300 W visible light, and 254 nm and 185 nm UV light.

Highlights

- 100% PFOA was degraded within 9 h by TiO_2/PMS under visible light
- 1.3:1 molar ratio of TiO_2/PMS was optimum for PFOA degradation
- $SO_4^{\bullet-}$ and photoinduced holes were the main active species
- 100% PFOA in real wastewater was degraded within 2 h under UV light

Declaration of interests

☒ The authors declare that they have no known competing financial interests or personal relationships that could have appeared to influence the work reported in this paper.

☐The authors declare the following financial interests/personal relationships which may be considered as potential competing interests: